Capturing of Drag Crisis by using Cartesian Coordinates System

Kunio Kuwahara (ISAS)

The Institute of Space and Astronautical Science

ABSTRACT

The flow around a bluff body is studied computationally at high Reynolds number to understand the mechanism of drag crisis and the transitional flow phenomena to turbulence.
It is found that simulation based on Cartesian coordinates system can capture the drag crisis. The present grid system is too coarse to resolve the boundary layer structure. This suggests that even the drag crisis phenomena are determined mainly by large structure of the flow field.

Key Words: drag crisis, Cartesian coordinates system, separation

1 Introduction

Flow around a bluff body is characterized by a strong vortex separation. This makes the flow turbulent in the wake. However, the mechanism of the separation leading to turbulence is not well understood because experimentally it is very difficult to see the very short period of the transition. It is also well known that, at high Reynolds number, the flow attaches well on the surface of the body if the surface is smooth. This causes sometimes unexpectedly low drag. This is called the drag crisis. In this paper, the flow around a bluff body is studied computationally at high Reynolds number to understand the mechanism of drag crisis and the transitional flow phenomena to turbulence.

Many of the high-Reynolds-number, turbulence simulations have been based on Reynolds-averaged Navier-Stokes equations using a turbulence model. Some use a large-eddy simulation. However, a usual turbulence model or a large-eddy simulation is not suitable for high-Reynolds-number-flow computation especially transitional phenomena. There are some real direct numerical simulation in which most of the small-scale structure are resolved, but the computations can be done only at relatively small Reynolds numbers.

In many applications, large structures are most important and we usually are not interested much about in small structures. What we want to do is to capture the large-scale structure using a coarse grid system.

Quite a few simulations (see Kuwahara, 1992), show that large structures of high-Reynolds-number, turbulent flow can be captured using relatively coarse grid, if the numerical instability, usually unavoidable for high-Reynolds-number-flow simulation, is suppressed. Most successful simulations in these approaches are based on the third-order upwind formulation (Kawamura and Kuwahara, 1984; Kuwahara, 1992; Kuwahara, 1999; Kuwahara and Komurasaki, 2001). An approach similar in philosophy but different in method is adopted by Boris et. al. (1992).

In the present paper, we simulated the flow around a bluff body with smooth surface to capture the drag crisis and the transition to turbulence, which is very difficult to compute by Reynolds averaged Navier-Stokes equations or by large-eddy simulation (Deardorff, 1970).

2 Computational method

The governing equations are the unsteady incompressible Navier-Stokes equations and the equation of continuity.

$$\mathrm{Div}\boldsymbol{v} = 0$$

$$\frac{\partial \boldsymbol{v}}{\partial t} + (\boldsymbol{v}\cdot\mathrm{grad})\boldsymbol{v} = -\mathrm{grad}p + \frac{1}{Re}\Delta\boldsymbol{v}$$

These equations are solved by a finite-difference method. The numerical procedure is based on the projection method (Chorin, 1968). Then, the pressure field is obtained by solving the Poisson equation.

All the spatial derivative terms are represented by the central difference approximation except for the convection terms. For the convection terms, the third-order upwind difference is used. This is the most important point for high-Reynolds-number computations.

There is another croucial problem in high-order upwind schemes. That is, the accuracy decreases when the flow direction is not well parallel to one of the coordinate lines. If we use generalized coordinate system, near the boundary, the flow direction and one of the coordinate lines are almost parallel, and this problem is not serious. However, in general, flow direction is not always parallel to a coordinate line and the problem become serious. To overcome this problem we introduced the multi-directional upwind method. This method is summarized as follows:

In case of 2-dimensional computation, when structured grid points are given, the black points in fig.1(a) are usually used to approximate the derivatives at the central point (system A).

If we introduce the other 45 degrees-rotated local grid points, the white ones in fig.1(b), which can be used to approximate the derivatives at the central point (system B).

In order to improve the derivative value at the central point, we mix the derivative values calculated from both systems (A and B) at a proper ratio. We adopt the ratio A : B = 2/3 : 1/3. Using this ratio, for example, resulting finite-difference scheme for the Laplacian coincides with the well-known 9-points formula with forth-order accuracy. This method improves the rotational invariance of the coordinate system. Then those flows where flow direction is not parallel to the grid direction are better simulated.

In case of 3-dimensional computation, we introduce three different grid systems. Each grid system is obtained by rotating ordinary one (system A) around one axis. For example, one of those systems, system B (x'-y'-z) is shown in fig.1.

In the same way as 2-dimensional computation, white circle points are used instead of black ones on the x-y plane, and ordinary ones in the z direction. Other grid systems are also introduced similarly. Thus we can obtain three different values at the same point, and they are averaged, since any physical phenomena are equivalent in each grid system. The rotational invariance of the coordinate system can be improved by means of this procedure.

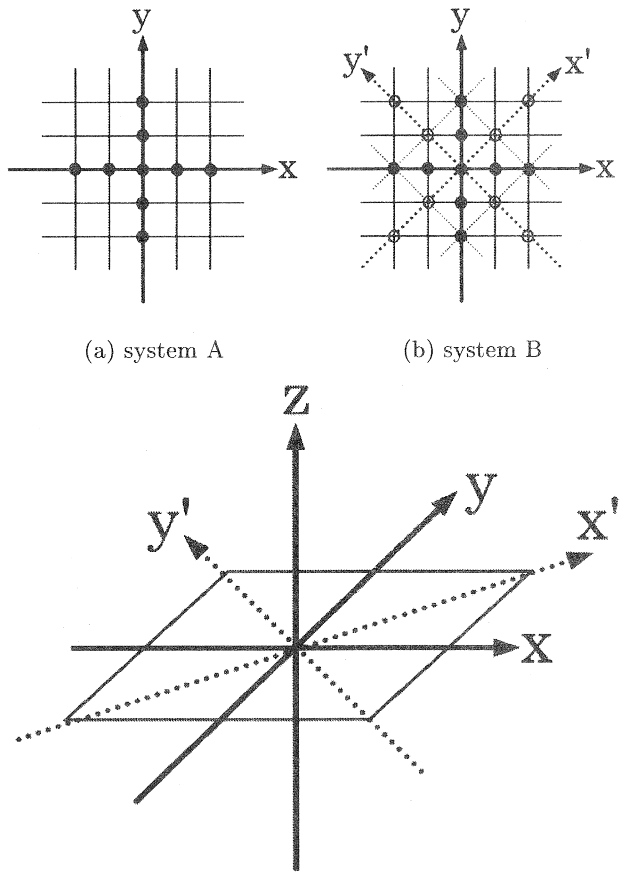

(c) system B: x'-y'-z

Figure 1 Grid for multi-directional scheme

For all the spatial derivatives, the multi-directional finite-difference method is used.

For the temporal integration of the Navier-Stokes equations, the Crank-Nicolson implicit scheme is utilized. This scheme has second-order accuracy in time. These equations and the Poisson equation are iteratively solved at each time step by the successive over relaxation (SOR) coupled with a multi-grid method.

3 Computational results

(1) Flow past a circular cylinder

The drag sharply decreases at about Reynolds number 400,000, which is called drag crisis, is well captured even using this coarse grid. Instantaneous and time-averaged flow patterns clearly show the difference as shown in Figs.2,3. After drag crisis, flow separation delays and the wake becomes narrower, which makes the drag less.

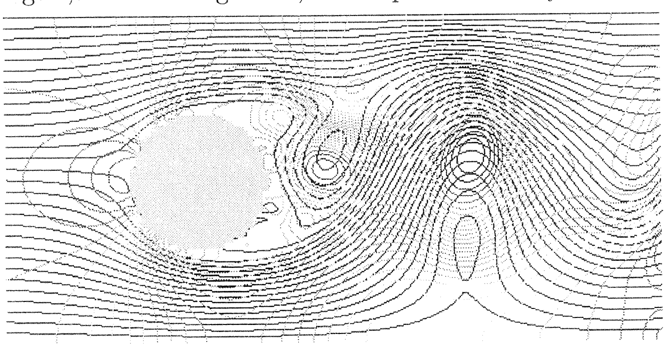

(a) Re = 10^4, before drag crisis

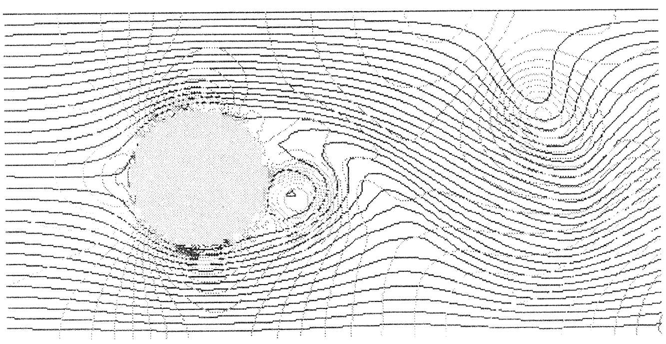

(b) Re = 10^6, after drag crisis

Figure 2 Instantaneous flow patterns;

stream lines, pressure contours, grid=129×65.

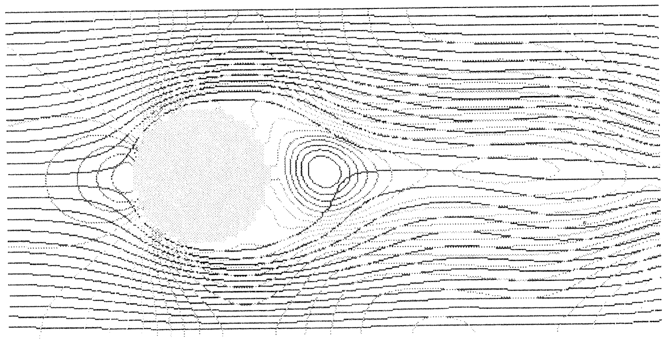

(a) Re = 10^4, before drag crisis

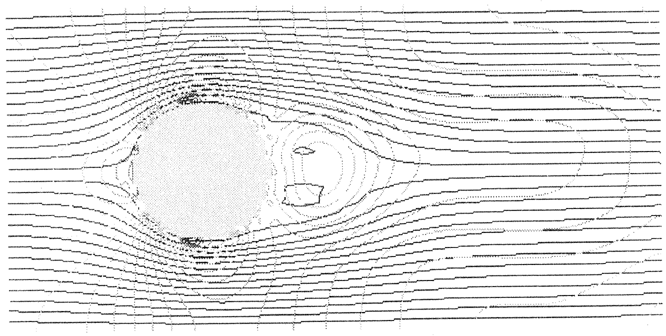

(b) Re = 10^6, after drag crisis

Figure 3 Time-averaged flow patterns;

stream lines, pressure contours, grid=129×65.

Results of finer computation at Re = 10^6 is shown in fig.4.

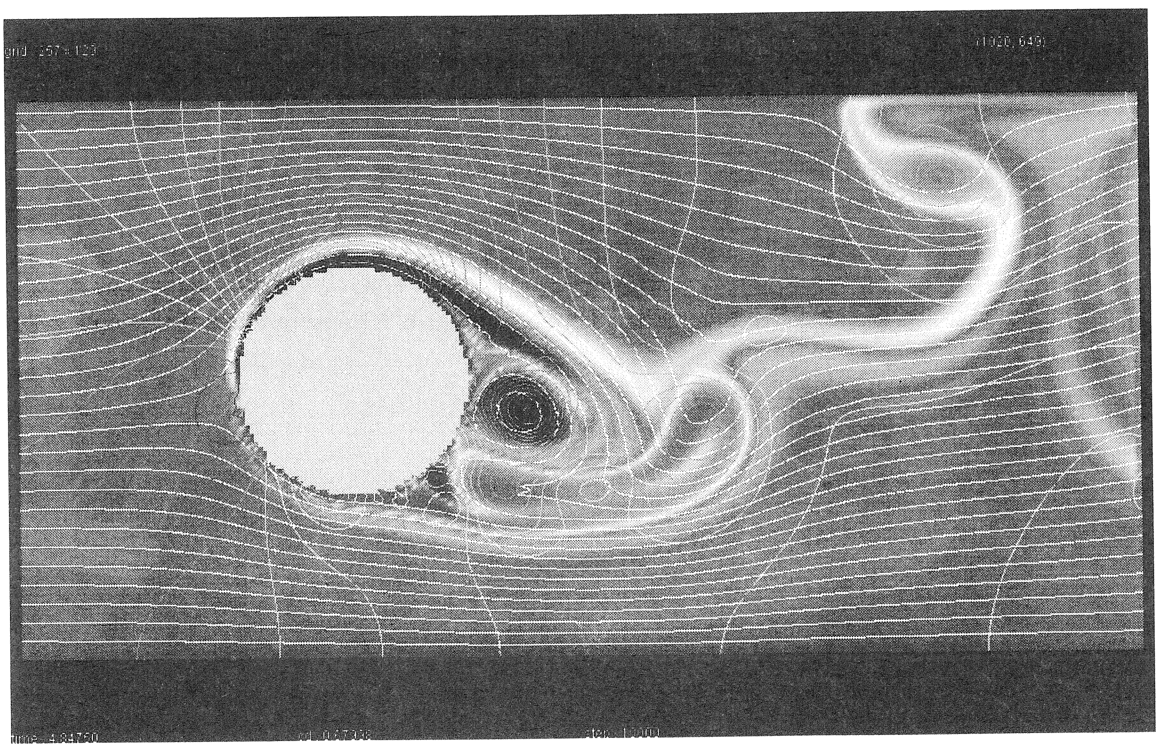

Figure 4 Instantaneous flow patterns; stream lines, pressure contours and vorticity shading.

(2) Flow past a sphere

Similar phenomena are observed in 3D computation. The simulation were carried out using two grid systems: $64 \times 32 \times 32$ and $128 \times 64 \times 64$. Even very coarse grid as $64 \times 32 \times 32$, can capture the drag crisis. Following figures show a flow around a sphere.

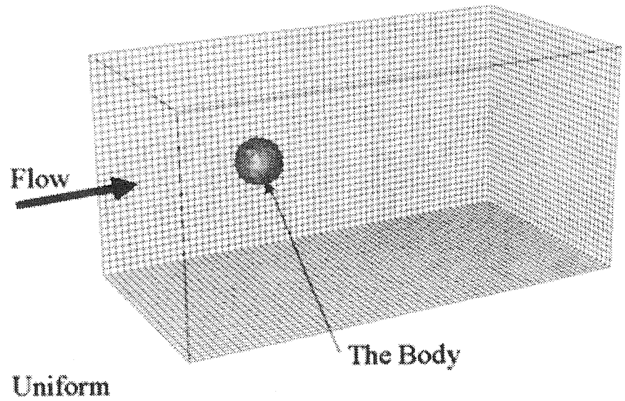

Figure 5 Computational grid for a flow around a sphere

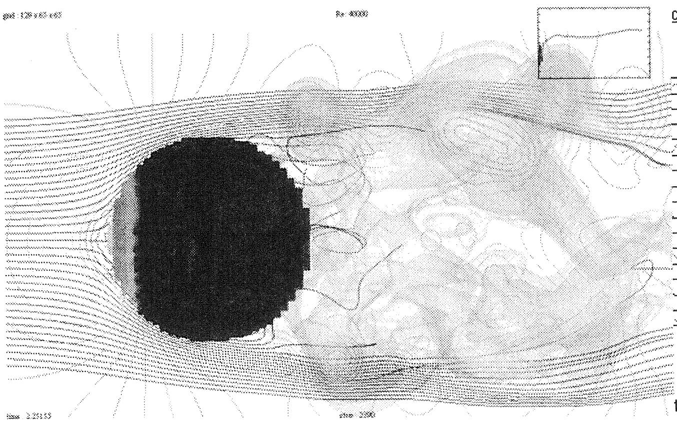

(a) Re $= 2 \times 10^4$, before drag crisis

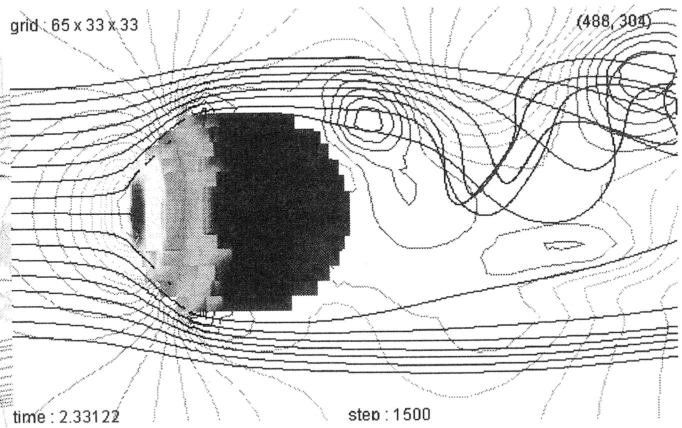

(a) Re $= 2 \times 10^4$, before drag crisis

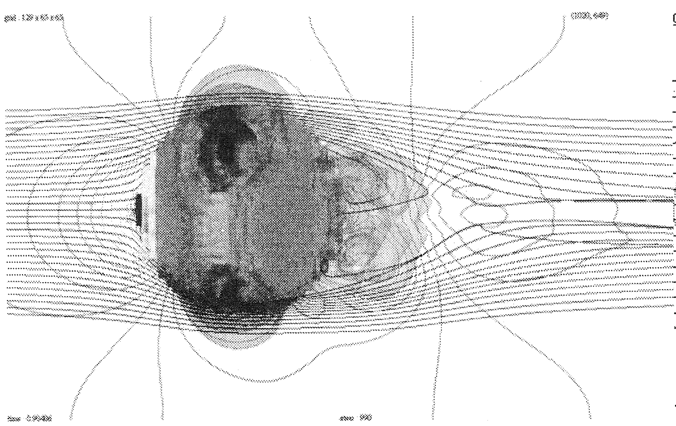

(b) Re $= 2 \times 10^6$, after drag crisis

Figure 6 Pressure contours and stream lines, grid $= 129 \times 65 \times 65$.

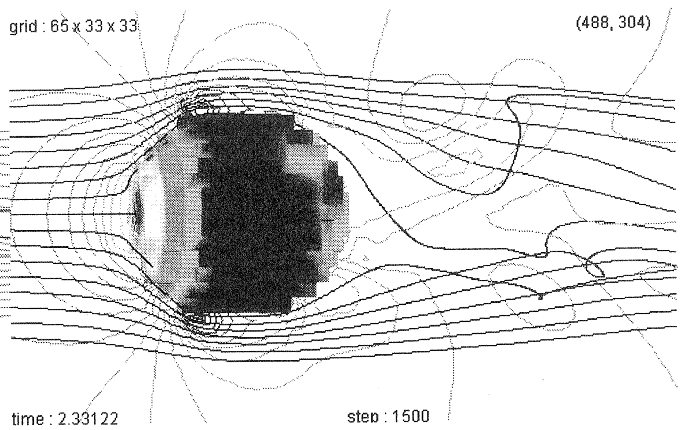

(b) Re $= 2 \times 10^6$, after drag crisis

Figure 7 Pressure contours and stream lines, grid $= 65 \times 33 \times 33$.

(3) Flow past an ellipsoid

Similar computation is done for a flow around an ellipsoid at Re=2,000,000, and Re=20,000. Figure 8 shows the flow patterns. The body shape is visualized by using CAD data directry.

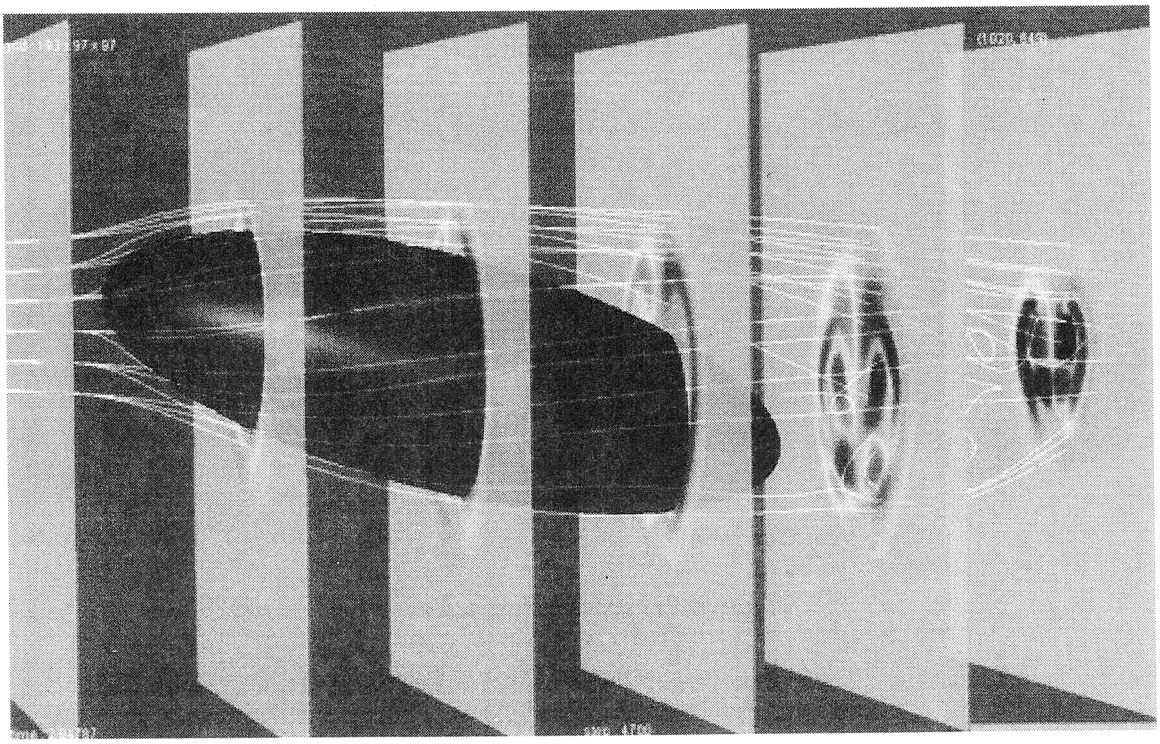

(a) Re $= 2 \times 10^4$, before drag crisis

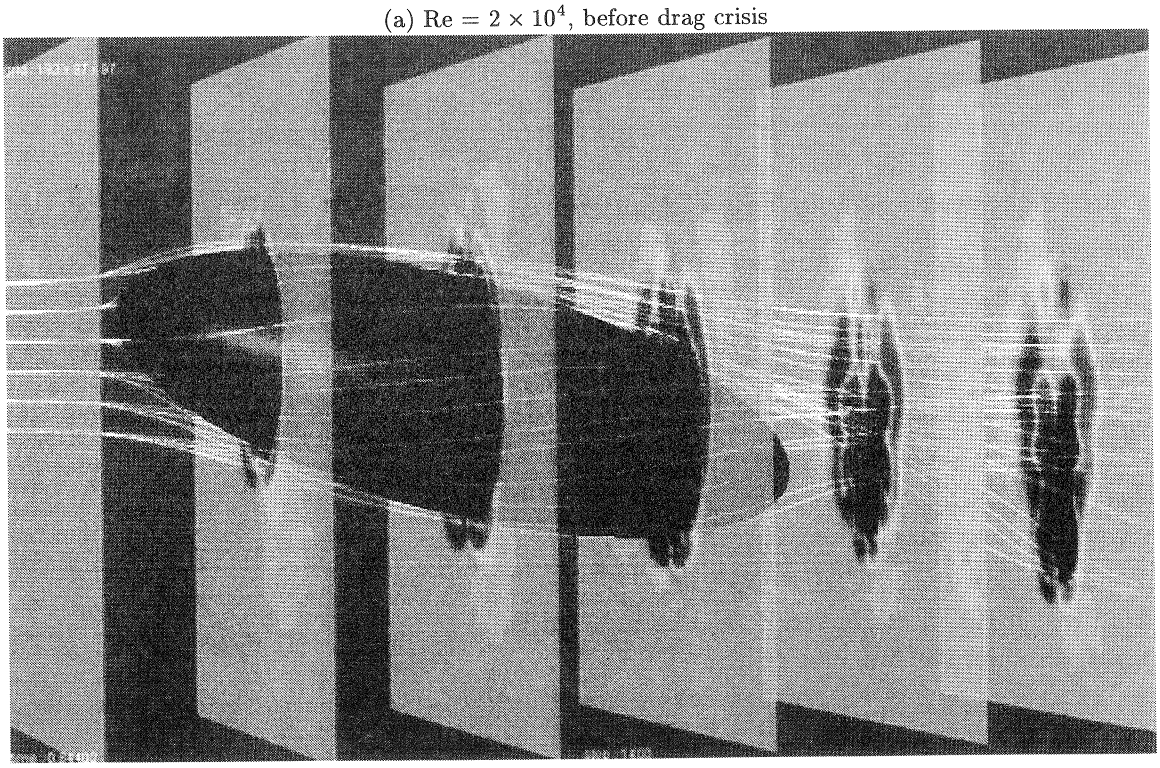

(b) Re $= 2 \times 10^6$, after drag crisis

Figure 8 Vorticity sharding and stream lines

(4) Flow around a car
As an example of more realistic case, a flow around a car is simulated. Following figures show the flow at Re=10,000,000.

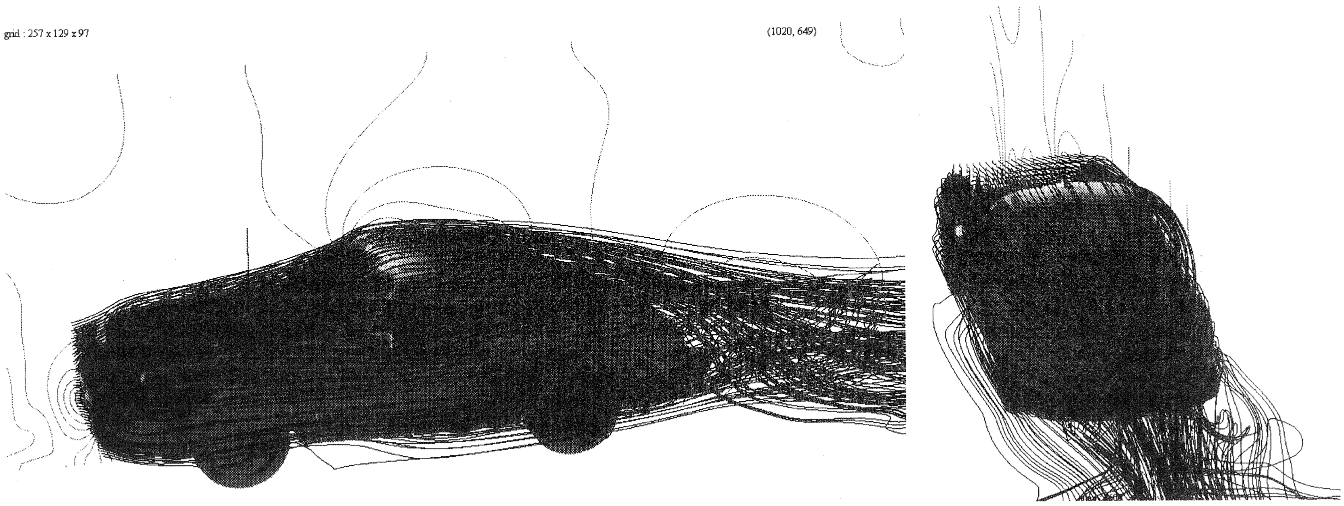

(a) Side view (b) Rear view

Figure 9 Pressure sharding and stream lines

4 Conclusion

It was found that simulation based on Cartesian coordinates system can capture the drag crisis. The present grid system is too coarse to resolve the boundary layer structure. This suggests that even the drag crisis phenomena are determined mainly by large structure of the flow field.

References

1) Boris, J.P., Grinstein, F.F., Oran, E.S. and Kolbe, R.L., 1992, "New insights into large eddy simulation," Fluid Dynamics Research 10, pp. 199-228
2) Chorin, A., J., 1968, Math. Comp. 22 pp. 745
3) Deardorff, J.W., 1970, "A Numerical Study of Three-Dimensional Turbulent Channel Flow at Large Reynolds Numbers," J. of Fluid Mechanics, Vol. 41, Part 2, pp. 453-480
4) Kawamura, T. and Kuwahara, K., 1984, "Computation of high Reynolds number flow around a circular cylinder with surface roughness," AIAA Paper 84-0340.
5) Kuwahara, K., 1992, "Flow Simulation on Supercomputers and Its Visualization," International Journal of High Speed Computing, Vol.4, No.1, pp. 49-70.
6) Kuwahara, K., 1999, "Unsteady Flow Simulation and Its Visualization," AIAA Paper 99-3405
7) Kuwahara, K. and Komurasaki, S., 2001, "Direct Simulation of a Flow around a Subsonic Airfoil," AIAA Paper 2001-2545